Acta metall. Vol. 31, No. 12, pp. 1977–1989, 1983
Printed in Great Britain.

0001-6160/83 $3.00 + 0.00

OVERVIEW NO. 33

INTERFACE CONTROLLED DIFFUSIONAL CREEP

E. ARZT[1], M. F. ASHBY[2] and R. A. VERRALL[3]

[1] Max-Planck-Institut für Metallforschung, Seestrasse 92, D-7000 Stuttgart, FRG,
[2] Cambridge University, Engineering Department, Trumpington Street, Cambridge CB2 1PZ, England
and
[3] Hoffman Laboratory, Harvard University, Oxford Street, Cambridge, MA 02138, U.S.A.

(*Received* 4 *March* 1983; *in revised form* 20 *May* 1983)

Abstract—Diffusional flow of a polycrystal is classically treated as a continuum diffusion problem: its rate is calculated by solving for the diffusional flux of matter through or around each grain in a polycrystal, driven by the stress acting on it. Many, but not all, experimental observations are adequately explained by this model. Progress in understanding the discrepancies can be made by considering the microscopic processes involved in diffusional flow: the detailed nature, and number, of sinks and sources in the grain boundaries; and their mobility. This paper treats these problems, and derives expressions for the rate of diffusional flow when the density of sinks and sources becomes small, and when their mobility is limited by impurities, solutes, or precipitates. The results become identical with those of the classical treatment in the appropriate limits.

Résumé—On traite classiquement l'écoulement diffusionnel d'un polycristal comme un problème de diffusion continue: on calcule sa vitesse en trouvant la solution pour un flux diffusionnel de matière à travers ou autour de chaque grain d'un polycristal, mû par la contrainte qui lui est appliquée. De nombreuses observations expérimentales, mais pas toutes, sont bien expliquées par ce modèle. On peut progresser dans la compréhension de ces différences en étudiant les phénomènes microscopiques impliqués dans le flux diffusionnel: la nature précise et le nombre des pièges et des sources intergranulaires, ainsi que leur mobilité. Cet article traite ces problèmes et nous obtenons des expressions pour la vitesse du flux diffusionnel lorsque la densité des pièges et des sources devient petite et lorsque leur mobilité est limitée par des impuretés, des atomes de soluté ou des précipités. Les résultats deviennent identiques à ceux du traitement classique dans les limites appropriées.

Zusammenfassung—Das Diffusionsfließen eines Polykristalles wird klassisch als ein Problem der Diffusion im Kontinuum behandelt: die Fließgeschwindigkeit wird berechnet, indem der Materie-Diffusionsfluß durch ein jedes Korn hindurch und daran vorbei ermittelt wird. Dieser Diffusionsfluß wird verursacht von Spannungen auf die Körner. Viele, allerdings nicht alle experimentelle Beobachtungen können mit diesem Modell erklärt werden. Das Verständnis der verbleibenden Diskrepanzen kann verbessert werden, wenn die beim Diffusionsfließen ablaufenden mikroskopischen Prozesse berücksichtigt werden. Hierzu gehören genaue Natur und Zahl von Senken und Quellen in den Korngrenzen, und die Beweglichkeit. In dieser Arbeit werden diese Probleme behandelt. Es werden Ausgrücke für die Geschwindigkeit des Diffusionsfließens für die Fälle abgeleitet, daß die Dichte von Senken und Quellen klein wird, und daß die Beweglichkeit durch Verunreinigungen, Legierungsatome und Ausscheidungen bestimmt ist. Die Ergebnisse gehen für entsprechende Übergänge in solche der kalssischen Behandlung über.

1. INTRODUCTION

1.1. *The need for an atomistic model for diffusional creep*

When stressed, a polycrystalline solid can deform plastically by the diffusion of single ions from one set of grain boundaries to another. When lattice diffusion controls the rate, the deformation is known as "Nabarro–Herring creep"; when, instead, transport is predominantly by grain boundary diffusion, it is common to call it "Coble creep". In fact, the two diffusional paths contribute simultaneously to the creep, and it is best to think of the combination as a single mechanism of deformation, which we will simply call *diffusional creep.*

The standard treatments of diffusional creep (cited below) are continuum calculations: a grain is treated as having a certain diffusive conductance (described by the lattice diffusion coefficient D_v) surrounded by a boundary layer of thickness δ with a higher diffusive conductance (described by the boundary diffusion coefficient D_b). Matter flows via these two paths from points of the grain surface on which compressive tractions act to points where the tractions are tensile (Fig. 1, left hand side). A basic unstated assumption is that *the entire grain boundary surface is a perfect sink or source for matter.* Then the rate of flow is determined only by the rate of diffusive transport from one part of the boundary to another.

This continuum treatment is remarkably successful. The constitutive law it predicts is in good agreement with many experiments on pure metals [1, 2]. But there exists a body of observations on pure metals and ceramics (Section 4.1), on impure metals and solid solutions (Section 4.2) and on alloys containing a fine dispersion of a second phase (Section 4.3) which cannot be explained by the theory as it stands. These include: creep-rates which are much slower than the continuum calculation predicts; a non-linear stress dependence of the creep-rate; activation energies which are too high; an unexpected dependence of creep-rate on grain size;

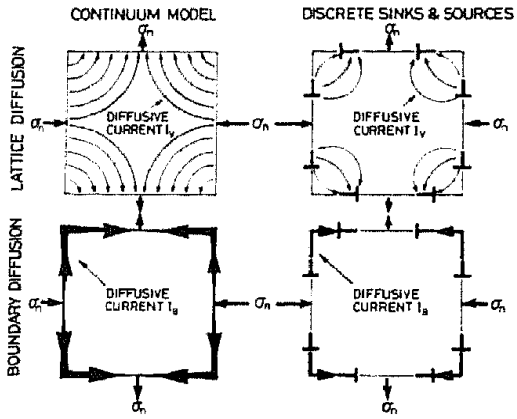

Fig. 1. The continuum model (left) contrasted with the discrete sink and source model (right).

and threshold stresses below which no detectable creep occurs.

The explanation of at least some of these discrepancies must lie in the details of how a grain or phase boundary acts as a sink or source for matter. Recent models for the structure of grain boundaries [3–8] suggest a fairly well defined structure that would be disrupted if atoms were removed from or added to it. This led to the suggestion [9–11] that the boundary surface as a whole does not act as a sink or source for matter, but that a divergence of the diffusive flux of matter can occur only at *boundary dislocations* which then move in a non-conservative way in the boundary plane (Fig. 1, right hand side). Electron microscopy [12, 13] reveals dislocations of the appropriate kind, in densities which vary with stress, up to about 10^7 m/m^2. Their Burgers' vectors are not lattice vectors, and therefore they are constrained to remain in the boundary when they move.

The continuum model of diffusional flow must now be modified in two ways. First, one must ask how the rate of diffusional creep is altered by the presence of discrete sinks and sources, and by their density (Section 2). And second—since the sinks and sources move during creep—one must ask how their mobility influences the creep-rate (Section 3).

The symbols used in the development are listed in Table 1.

Table 1. Table of symbols

d	grain size (m)
T_M	melting temperature (K)
G	shear modulus (N/m^2)
Ω	atomic volume (m^3)
D_v	lattice diffusivity (m^2/s)
δ	boundary thickness (m)
D_b	grain boundary diffusivity (m^2/s)
D_i	diffusivity in particle boundary (m^2/s)
D_{eff}	effective diffusivity for diffusional creep (eq. 2) (m^2/s)
D_s	diffusivity of solute or impurity atoms (m^2/s)
b	Burgers' vector of lattice dislocation (m)
b_b	Burgers' vector of grain boundary dislocation (m)
b_n	component of b_b normal to the boundary plane (m)
N_A	number of particles per unit area of grain boundary (m^{-2})
N_V	number of particles per unit volume (m^{-3})
r	particle radius (m)
l	spacing of dispersed particles ($=1/\sqrt{N_A}$) (m)
$\gamma, \dot{\gamma}$	shear strain, shear strain rate (−, s^{-1})
$\varepsilon, \dot{\varepsilon}$	tensile strain, tensile strain rate (−, s^{-1})
σ_s, σ_{tr}	shear stress, threshold stress in shear (N/m^2)
σ, σ_0	tensile stress, threshold stress in tension (N/m^2)
σ_n	normal traction acting on grain boundary (N/m^2)
σ_i	equilibrium stress at ith grain boundary dislocation (N/m^2)
μ	chemical potential (J)
v_{dis}	velocity of grain boundary dislocation (m/s)
N	number of grain boundary dislocations per grain face
ρ	surface density of grain boundary dislocation $= N/d$ (m^{-1})
E_s	self energy of dislocation per unit length (J/m)
M	mobility of grain boundary dislocation (m^2/Ns)
M_i	mobility of gb-dislocation in particle/matrix interface (m^2/Ns)
n_s	number of solute atoms per unit length of dislocation (m^{-1})
α_0	infinitesimal length change per unit advance of gb-dislocation in pure material
β	segregation coefficient for solute atoms around a dislocation
C_0	solute concentration
C_1, C_2, C_3, C_4	constants of order 1
n_c	number of particles, per unit length of dislocation, that are by-passed by climb/glide in the particle/matrix interface (m^{-1})
n	number of particles per unit length of dislocation ($=1/l$) (m^{-1})

1.2. *The continuum solution*

Before proceeding to the microscopic models, we cite the generally-accepted continuum solution for the rate of diffusional creep [14–19]. If the grain boundaries act as perfect sinks and sources so that creep is *diffusion controlled*, then a shear stress σ_s produces a shear strain-rate $\dot{\gamma}$ given by

$$\dot{\gamma} = \frac{C\Omega D_{\text{eff}}}{kTd^2}\sigma_s. \tag{1}$$

Here C is a constant equal to about 40, Ω is the atomic or molecular volume, d the grain size, k is Boltzmann's constant, T the absolute temperature and D_{eff} is an effective diffusion coefficient given by

$$D_{\text{eff}} = D_v\left(1 + \frac{\pi\delta D_b}{dD_v}\right) \tag{2}$$

where D_v is the diffusion coefficient for mass transport through the lattice, and δD_b the boundary thickness times the diffusion coefficient for mass transport in the grain boundary. For simple tension, this constitutive law becomes

$$\dot{\varepsilon} = \frac{C\Omega D_{\text{eff}}}{3kTd^2}\sigma \tag{3}$$

where $\dot{\varepsilon}$ is the tensile strain-rate and σ the tensile stress.

2. THE DISCRETE SINK AND SOURCE MODEL: DIFFUSION CONTROL

Figure 2 shows a square grain acted on by equal, opposite, normal tractions σ_n, at a temperature at which self-diffusion can occur rapidly. The grain boundaries

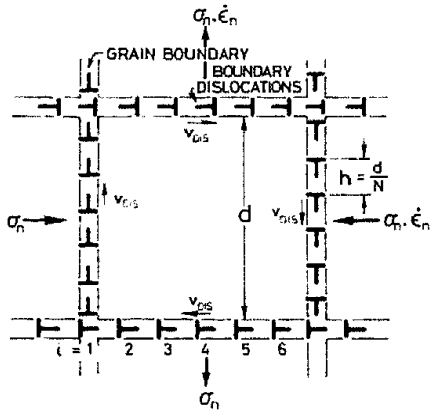

Fig. 2. Model of a grain under stress, showing the boundary dislocations which climb as creep takes place.

contain an array of straight, parallel grain boundary dislocations of spacing h. The array extends to infinity (or to the sample surfaces). When the boundary acts as a sink or source of matter, the dislocations climb in the boundary; if one is lost at one grain corner (at steady state), another is gained at another, so that the number, per grain face, remains constant. Matter can be released or absorbed only at the cores of the boundary dislocations. In this section we consider how the discrete nature of these sinks and sources changes the creep rate—assuming that their mobility is high. In Section 3, we consider what happens when their mobility is limited.

2.1. *Grain boundary diffusion*

When transport is by boundary diffusion—the most important case—the problem, given certain assumptions, can be solved exactly. We assume, first, that the core of a boundary dislocation is a perfect source or sink for matter; that is, that the chemical potential of matter in the immediate vicinity of a dislocation is that which is in equilibrium with the core of a straight dislocation, acted on by the local boundary traction, σ_n. Using the same definitions and symbols as Herring [15] we have that

$$(\mu-\mu_v) = \mu_0-\sigma_n\Omega \tag{4}$$

where μ is the potential of matter, μ_v that of vacancies and μ_0 that of matter in a standard, stress-free crystal. It is gradients of $(\mu-\mu_v)$ which drive the diffusive flux of matter. Figure 3 shows schematically the distribution of $(\mu-\mu_v)$ in a boundary: it varies linearly between dislocations because there are no sources or sinks there.

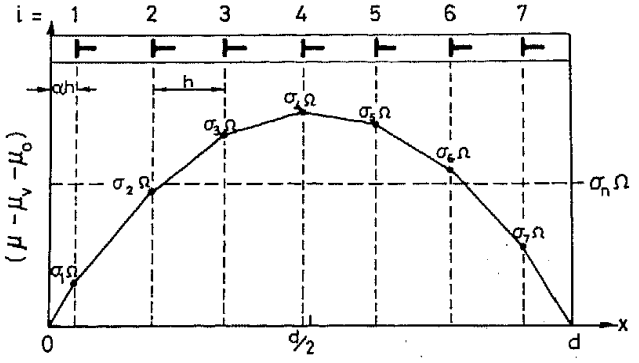

Fig. 3. The variation of chemical potential with position across one grain facet when transport is by boundary diffusion.

Second, we assume that the dislocations are evenly spaced, so that they all climb at the same speed. In the infinite array of dislocations of which Figs 2 or 3 is a part, a dislocation which is out of place experiences a force tending to restore the even spacing. Local barriers to dislocation movement—precipitates, for instance—may disturb it, but we postpone discussion of this to Section 3.

Consider the motion of the ith dislocation of Fig. 3. Its velocity of climb, v_{dis} is determined by the difference in the current of matter (atoms/unit length/second) arriving at its core from its left, I_L, and leaving on its right, I_R. Then

$$v_{dis} = \frac{(I_R-I_L)\Omega}{b_n} \tag{5}$$

where b_n is the component of the Burgers' vector of the grain boundary dislocation normal to the boundary plane. The current to the right is given by

$$I_R = \frac{D_b\delta}{\Omega kT}\nabla\mu = \frac{D_b\delta}{\Omega kT}\left(\frac{\sigma_{i+1}\Omega-\sigma_i\Omega}{h}\right) \tag{6}$$

and that from the left is

$$I_L = \frac{D_b\delta}{\Omega kT}\left(\frac{\sigma_i\Omega-\sigma_{i-1}\Omega}{h}\right) \tag{7}$$

where σ_i etc. are the local normal tractions acting on the boundary at the site of the ith dislocation.

Assembling these results gives, for $i = 2$ to $N-1$,

$$v_{dis} = \frac{\delta D_b\Omega}{b_n kT}\left\{\frac{\sigma_{i+1}-2\sigma_i+\sigma_{i-1}}{d/N}\right\} \tag{8}$$

where $N = d/h$ is the number of dislocations in a single grain wall.

If the first dislocation is a distance αh from the grain corner, and the last is a distance $(1-\alpha)h$ from its corner, then equilibrium requires that

$$\sum_2^{N-1}\sigma_i+\sigma_1\left(\frac{1+\alpha}{2}\right)+\sigma_N\left(\frac{2-\alpha}{2}\right) = \sigma_n N. \tag{9}$$

By symmetry, the chemical potential at the grain corners must be zero, and all the dislocations move at the same velocity, which requires that

$$\sigma_2-\sigma_1\left(1+\frac{1}{\alpha}\right) = \sigma_{N-1}-\sigma_N\left(1+\frac{1}{1-\alpha}\right) \tag{10}$$

and

$$\sigma_{i+1}-2\sigma_i+\sigma_{i-1} = \sigma_2-\sigma_1\left(1+\frac{1}{\alpha}\right). \tag{11}$$

The solution to this set of equations is

$$\sigma_i = Ai^2+Bi+C$$

where

$$A = \frac{6\sigma_n}{1-N^2-6\alpha+6\alpha^2}$$

$$B = \frac{-6\sigma_n(N-2\alpha+2)}{1-N^2-6\alpha+6\alpha^2} \tag{12}$$

$$C = \frac{6\sigma_n[2\alpha^2-(N+3)\alpha+N+1]}{1-N^2-6\alpha+6\alpha^2}$$

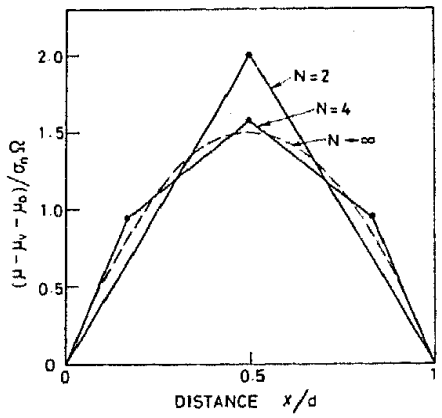

Fig. 4. Plot of equation (12) showing the variation of chemical potential with dislocation number N. The limit at $N = \infty$ is a parabola, in agreement with the continuum model.

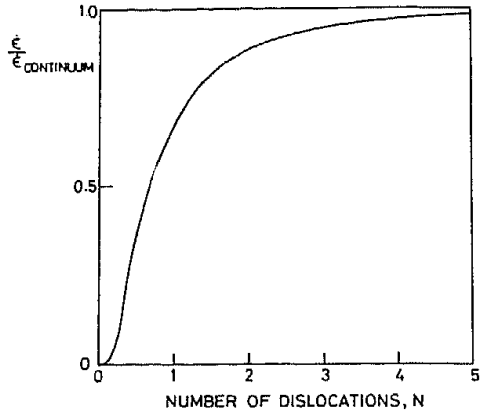

Fig. 5. Plot of equation (21) showing the reduction in creep rate caused by a low density of boundary dislocations.

In the continuum limit of large N, the discrete variable (ih) is replaced by the continuous variable x, such that

$$\sigma(x) = \frac{6x}{d}\left(1-\frac{x}{d}\right)\sigma_n \tag{13}$$

giving a parabolic stress distribution at steady state (in agreement with the result of Lifshitz [16] and Raj and Ashby [19]). But as N becomes small, it is necessary to describe the stress distribution by the discrete series given by equation (12). It is shown in Fig. 4.

The dislocation velocity is given by substituting equation (12) into equation (8). The result is

$$v_{\text{dis}} = \frac{\delta D_b \Omega}{b_n kT}\frac{N}{d}\left(\frac{12\sigma_n}{N^2-1+6\alpha-6\alpha^2}\right). \tag{14}$$

It is a minimum when $\alpha = \frac{1}{2}$. The creep rate $\dot{\varepsilon}_n$ (Fig. 2) is

$$\dot{\varepsilon}_n = \frac{\rho b_n v_{\text{dis}}}{d} \tag{15}$$

where ρ is the surface density of boundary dislocations ($\rho = N/d$). Inserting the minimum value of equation (14) and noting that, for the stress state of Figs 1 and 2, $\sigma_s = \sigma_n$ and $\dot{\gamma} = 2\dot{\varepsilon}_n$ we find

$$\dot{\gamma} = \frac{24\delta D_b \Omega \sigma_s}{kTd^3}\left\{\frac{N^2}{N^2+\frac{1}{2}}\right\} \tag{16}$$

In the continuum limit (N large) the term in curly brackets reduces to unity, and the expression is almost identical with the classical Coble creep equation. The only difference is the constant, 24; the calculations cited earlier predict about 40. This difference is a consequence of the idealised grain shape used here (which permits no sliding) and our definition of grain size. The important term is that in curly brackets: it describes the slowing-down process of diffusional flow caused by a limited number (N per grain) of discrete sources and sinks. It is plotted in Fig. 5.

2.2. *Lattice diffusion*

When lattice diffusion contributes, the problem becomes more complicated. Even when boundary diffusion is not the dominant transport mechanism, it still smears out the localized character of the sinks and sources. Instead of a point source (in the two-dimensional picture of Fig. 2) each dislocation becomes a line source broadened in the boundary plane. If these lines overlap, the discrete nature of the sources and sinks is lost.

The breadth, Z, of the boundary sources is the mean free path of an atom in the boundary before leaving it and entering the bulk of the crystal. It is given by [20]

$$Z = \sqrt{2}a\exp\left(\frac{\Delta Q}{RT_M}\frac{T_M}{T}\right) \tag{17}$$

where $\Delta Q = Q_v - Q_b$ and Q_v is the activation energy for lattice diffusion and Q_b that for boundary diffusion; a is the atom size. The dimensionless quantity $\Delta Q/RT_M$ has a value between 6 and 10 for almost all the materials for which data are available [21]. Taking 8 as typical, the broadening Z/a decreases from 10^7 (or $Z \approx 2$ mm) at 0.5 T_M to 4×10^3 (or $Z \approx 1$ μm) at the melting point. This means that, unless N is small, the boundary will act as a nearly perfect sink and source for lattice diffusion at all but the highest temperatures.

2.3. *Threshold stresses in pure metals and ceramics*

A boundary dislocation (like a lattice dislocation) cannot end within the solid. It must either be continuous, or link, at nodes, to one or more other dislocations such that the sum of the Burgers' vectors flowing into the node is zero. If this continuous line now tracks across the irregular surface making up the boundary between grains (Fig. 6) its overall length fluctuates, and the nodes move along the length of the dislocation line.

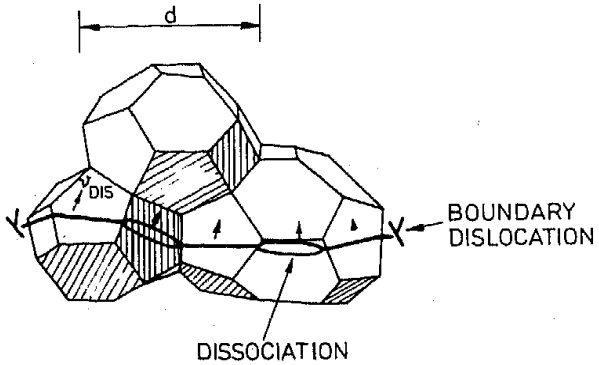

Fig. 6. A boundary dislocation on a grain boundary surface.

Let the self energy, per unit length, of a boundary dislocation be

$$E_s \approx \frac{Gb_b^2}{2} \tag{18}$$

where b_b is the magnitude of the Burgers' vector of the boundary dislocation. If the dislocation segment of length d moves a distance d over the grain surface, its length fluctuates (and the nodes move) by a distance which is proportional to d; let this be $\alpha_0 d$ (where $\alpha_0 \approx 0.2$). Then, equating the work done by the applied stress σ_n to the energy change for a length d of dislocation gives

$$\sigma_n b_n \frac{d^2}{2} = \alpha_0 d E_s. \tag{19}$$

This process occurs on both the source-boundaries and those which act as sinks. The result is a threshold stress in simple tension of

$$\sigma_{tr} = \frac{2\sqrt{2}\alpha_0 G b_b}{d} \tag{20}$$

(where we have set $b_b/b_n = \sqrt{2}$. As a value for b_b we take one third of a lattice dislocation Burgers' vector). It has magnitude for 10 μm grains, of roughly $\sigma_0/G \approx 10^{-5}$. Data for threshold stresses are tabulated in Section 4. They are of this general magnitude in pure metals.

An expression with the same form as equation (20) was derived by Burton [22] using the idea that a spiral boundary source, in operation, must acquire a radius of curvature equal to half the grain size.

2.4. Conclusions: influence of discrete sinks and sources on diffusional creep in pure materials

When the discrete nature of sinks and sources is allowed for in calculating the rate of diffusional creep, it is found that a correction factor must be applied to the usual constitutive law [equations (1) or (3)]. This factor, for boundary-diffusion control, is

$$\phi = \left(\frac{N^2}{N^2 + \frac{1}{2}}\right) \tag{21}$$

where N is the number of boundary dislocations per grain face. Unless this number is very low ($N \approx 1$), the correction is close to unity (Fig. 5). For lattice-diffusion control, diffusive broadening makes the factor even closer to 1.

This is probably why measurements of diffusional flow in pure materials are often well described by the continuum equation (1) or (3). But the presence of line defects which move when the boundary acts as a sink or source has one important consequence: because the defects move, their line length (and the associated energy) fluctuates; this fluctuation leads to a lower-limiting threshold stress for diffusional flow which, in simple tension, is about

$$\sigma_{tr} \approx \frac{1}{2}\frac{Gb_b}{d} \tag{22}$$

3. THE INFLUENCE OF DISLOCATION MOBILITY (THE "INTERFACE REACTION")

When boundary dislocations move easily, diffusion determines the creep-rate. But if a viscous drag, or a friction, or a pinning force, opposes the motion of the dislocations, then the material may creep more slowly. When this is so, the creep is said to be "mobility-limited" or "interface-reaction controlled" because its rate is determined by local processes taking place at the interface (the grain boundary) rather than by the kinetics of long-range diffusion. Aspects of this idea have been developed by Ashby [9, 10], Greenwood [23], Burton [22, 24], Harris [25], Burton and Beeré [26, 27] and Clegg and Martin [28], but no comprehensive treatment is available.

3.1. General rate-equation for diffusional creep with limited dislocation mobility

When mobility is limited, creep involves two dissipative processes: the motion of the dislocations against a drag force, and the diffusive transport of atoms across the grain. These are not alternative processes; both are necessary. The rate-equation can be derived by equating the external work-rate ($\sigma\dot{\varepsilon}$ per unit volume) to the sum of the powers dissipated in the two processes. This is equivalent to forming the harmonic mean of the strain-rates of each, acting alone

$$\frac{1}{\dot{\varepsilon}} = \frac{1}{\dot{\varepsilon}_{\text{diff}}} + \frac{1}{\dot{\varepsilon}_{\text{mobility}}}. \tag{23}$$

For simple tension $\dot{\varepsilon}_{\text{diff}}$ is given by equation (3). The dislocation velocity is related to the force $F = \sigma_n b_n$ per unit length acting on it, and to its *mobility* M, by

$$v_{\text{dis}} = MF. \tag{24}$$

Using equation (15) and converting to simple tension, we obtain

$$\dot{\varepsilon}_{\text{mobility}} = \frac{2}{3}\frac{M\rho b_n^2 \sigma}{d} \tag{25}$$

where ρ is the density of boundary dislocations. The resulting rate-equation for simple tension is

$$\dot{\varepsilon} = \frac{\dfrac{C\Omega D_{\text{eff}}\sigma}{3kTd^2}}{1 + \left[\dfrac{C\Omega D_{\text{eff}}}{2kTM\rho b_n^2 d}\right]}. \tag{26}$$

This is the basic rate-equation for diffusional creep including the effect of the interface reaction [9]. To proceed further, we must develop explicit expressions for M.

3.2. Solid solution strengthening in diffusional creep

A solid solution, or dissolved impurities, influence diffusional creep in two ways. First, the proper diffusion coefficient for mass transport depends on the concentration and diffusion coefficients of the components. When the stress is first applied,

components with different mobilities move at different rates, so that concentration gradients appear across grains. In ionic solids, even a slight difference in mobility between cation and anion causes charge separation: the resulting field slows the faster moving species and speeds up the slower until, at steady state, all move at the same speed. In metallic alloys, the concentration gradients may be larger, but their effect is the same: at steady state all species move at the same speed. The general expression for the steady-state flux of an atomic species in a solid containing n species is given by Lazarus [29]. In a solution containing atom fractions C_A and C_B of components A and B, the diffusion coefficient for mass transport is

$$D_v = \frac{D_v^A D_v^B}{C_A D_v^B + C_B D_v^A} \tag{27}$$

where D_v^A and D_v^B are the tracer diffusion coefficients of the individual species. An analogous expression holds for the grain-boundary diffusion coefficient.

But a steady-state may not be reached. If grain boundaries migrate into fresh crystal as diffusional creep progresses, leaving a zone of changed composition in their wake, then faster creep, at a rate largely determined by diffusion of the faster moving species, becomes possible [30]. The appropriate diffusion coefficient is then

$$D_v = C_A D_v^A + C_B D_v^B. \tag{28}$$

An analogous expression holds for the grain boundary diffusion coefficient.

The second, and more important, influence of a solid solution is a consequence of the dislocation-like character of the sinks and sources. Solute or impurity atoms that differ from the host atoms in size, compressibility, or charge, will redistribute themselves in the strain field of each dislocation, as illustrated in Fig. 7. The segregant exerts a drag on the dislocation, limiting its mobility.

Let the excess number of impurity or solute atoms, per unit length, be n_s; and let v_{dis} be the steady state velocity of all dislocations, and F_s be the force exerted by a dislocation on a single solute atom. Then if the solute moves with the dislocation, the force F_s must satisfy the Einstein mobility equation

$$v_{dis} = \frac{D_s}{kT} F_s \tag{29}$$

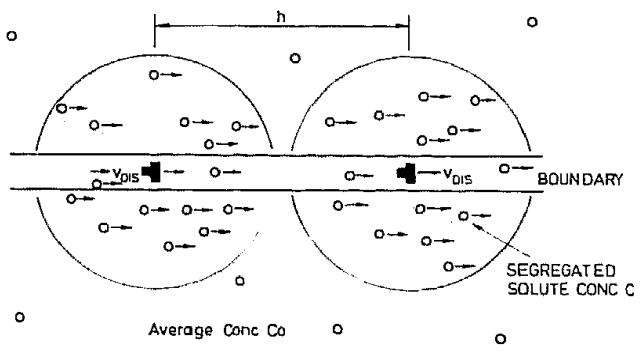

Fig. 7. Impurities or solute around a grain boundary dislocation. For modest binding energies, U, the segregated zone is within a radius of a few b of the dislocation core.

where D_s is the diffusion coefficient for the solute (D_s/kT is the *solute* mobility). Each solute atom exerts an equal but opposite force on the dislocation so that

$$F = n_s F_s \tag{30}$$

and the dislocation velocity v is

$$v_{dis} = \left(\frac{D_s}{kTn_s}\right) F. \tag{31}$$

The term in brackets is the *dislocation* mobility, M.

Calculation of n_s are given by Cottrell and Jaswon [31] and Cottrell [32]. Their calculations, much simplified, indicate that the segregation is localised to a cylinder of radius of a few b, within which the local concentration C_d is

$$C_d = C_0 \exp \frac{U}{kT} \tag{32}$$

where C_0 is the overall solute concentration and U is the binding energy per atom. Then n_s is given by

$$n_s \approx \frac{b_b^2}{\Omega} C_d = \frac{b_b^2}{\Omega} C_0 \exp \frac{U}{kT}. \tag{33}$$

The binding energy U at 1000°C is typically [33] 1 to 3 kT giving

$$n_s \simeq \frac{\beta b_b^2 C_0}{\Omega} \tag{34}$$

where β is between 3 and 20. We then find

$$M = \frac{D_s \Omega}{\beta k T b_b^2 C_0}. \tag{35}$$

The dislocation mobility increases with purity (an upper limit at $C_0 = 0$ is set by the intrinsic mobility $D_b b/kT$). It is severely restricted when C_0 is large.

To proceed further, we need an expression for the boundary dislocation density, ρ. It is generally proposed [34, 22] that

$$\rho = \frac{C_1 \sigma}{G b_b} \tag{35}$$

where $C_1 \approx 0.5$ (this being the planar equivalent of the equation $\rho = C_2 \sigma^2 / G^2 b^2$ describing the dislocation density within the grains). Then the creep-rate, equation (26), becomes

$$\dot{\varepsilon} = \frac{\dfrac{C \Omega D_{eff} \sigma}{3kTd^2}}{\left(1 + \dfrac{C\beta}{2C_1} \dfrac{C_0 G b_b}{d\sigma} \dfrac{D_{eff}}{D_s}\right)}. \tag{37}$$

In the diffusion controlled limit, this reduces to the continuum equation (3); but in the mobility-controlled limit, it becomes the equation for *solute-drag limited diffusional creep*

$$\dot{\varepsilon}_{mobility} = \frac{2 C_1 \Omega \sigma^2 D_s}{3 \beta k T b_b G C_0 d}. \tag{38}$$

Then the creep-rate varies as σ^2 and inversely as d. Note that this limit is the important one when

$$\frac{C\beta}{2C_1}\frac{C_0 G b_b}{d\sigma}\frac{D_{\text{eff}}}{D_s} > 1 \tag{39}$$

that is, when impurity levels are high, grains are small, and when temperatures are relatively low. When it is, the activation energy is that for solute diffusion.

3.3. *Particle hardening in diffusional creep*

Several theories of the influence of particles on diffusional creep have been put forward, but none has gained general acceptance. Because diffusion rates are not affected by a small volume fraction of inert particles, attention has focussed on the vacancy absorption and emission on grain boundaries (the "interface reaction").

Harris [25] assumes that vacancies are deposited and emitted only at the grain boundaries but not in the particle/matrix interface. The stress in the interface increases until the nucleation of dislocation loops relaxes it. This leads to a threshold stress, given by

$$(\sigma_{tr})_H = \frac{Gb}{r} f \tag{40}$$

where b is the lattice Burgers' vector, f the volume fraction of particles and r their radius. Such punching seems unlikely at the high temperatures of diffusional flow (and loops have not been observed). Other ways of relaxing the stress at the particles are discussed by Burton [24], and Burton and Beeré [26]. The alternative explanation [9, 10] is that vacancies can be absorbed and emitted only at grain boundary dislocations; particles pin the grain boundary dislocations (just as they do within the grain), and a threshold stress must be exceeded to make them move.

Consider a boundary surface which contains stable particles, or voids, or other *discrete obstacles* (Figs 8 and 9). In general, a boundary dislocation will interact with discrete obstacles which have a modulus, or lattice parameter, or chemical composition which differs from that of the matrix. The interaction energy can be negative (as with a void) or positive (as with a hard particle); in either case, the energy of the dislocation changes as it by-passes the obstacle, which therefore exerts a pinning force K (equal to the derivative of the

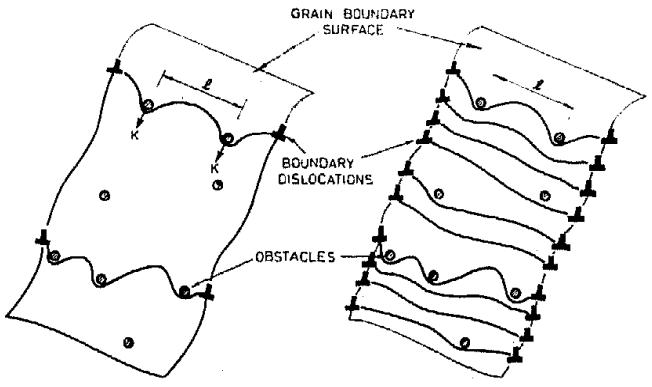

Fig. 8. Boundary dislocations interacting with discrete obstacles in a grain boundary, single dislocations (left) and dislocation pile-ups (right).

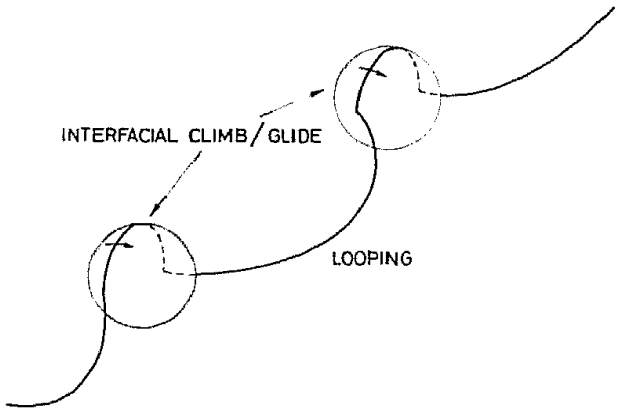

Fig. 9. The details of the interaction of Fig. 8.

energy with respect to distance) on it. This force must be overcome if the dislocation is to move, and leads to the true *threshold stress* below which diffusional creep stops. If the intrinsic mobility of the dislocation in the particle/matrix interface is *high*, then the pinning force can be calculated. The calculation requires the adaptation to high temperatures and to grain boundary dislocations of the classic Orowan calculation of the pinning of lattice dislocations by hard particles. It gives the stress required to break a dislocation free of particles of spacing l as

$$\sigma_{\text{Or}} = \frac{C_3 Gb}{l} \tag{41}$$

where $C_3 \approx 0.8$. The adaptation to high temperatures (when climb is possible) has been treated numerically by Shewfelt and Brown [36] and analytically by Arzt and Ashby [37]. The result is simple: it is that the particles introduce a threshold stress which is less than the Orowan stress by a factor of about 0.4. We thus have, for boundary dislocations, the threshold stress in shear of

$$\sigma_{tr} \approx \frac{0.3 G b_b}{l}. \tag{42}$$

This σ_{tr} is roughly a factor of 10 smaller then σ_{Or} because $b_b \approx \frac{1}{3}b$

But this alone does not account for the observed effect of particles on diffusional flow. There is evidence for a second effect. When a dislocation moves in a grain boundary, its local or intrinsic mobility is determined by the kinetics of atom rearrangement in the boundary, and can be calculated [10]; it is

$$M = \frac{C_4 D_b b_b}{kT} \tag{43}$$

(in unit of m^2/sN) where C_4 is a constant of about unity. When dislocations climb in clean grain boundaries, this intrinsic mobility is so great that it does not limit the creep rate, which is controlled, instead, by long-range diffusion across the grains. But when the dislocation moves in the particle–matrix interface, it appears that its local mobility is limited by the kinetics of atom rearrangement in the particle or the matrix *whichever is*

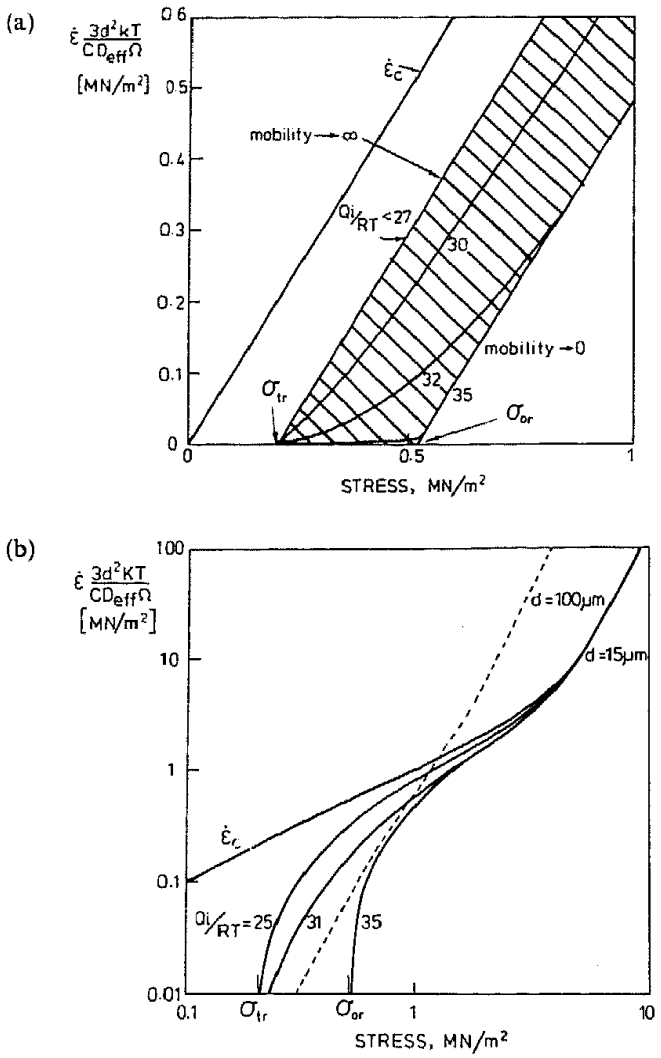

Fig. 10. The influence of grain boundary particles on the stress dependence of diffusional creep, as prediced by equations (A5)–(A8). The parameter shown is Q_i/RT, where Q_i is the activation energy for interfacial motion of a dislocation, d is the grain size, $\dot{\varepsilon}_c$ is the continuum solution. (a) Linear plot, (b) double logarithmic plot, where power-law creep is included at high stresses.

slower. It is given by

$$M = \frac{C_4 D_i b_b}{kT} \tag{44}$$

where D_i is a coefficient characterising atom rearrangement in the particle–matrix interface. Measurements of particle-motion in a force-field; of particle-dragging by grain boundaries [38] and of diffusional creep in dispersion-hardened materials (see Table 4) all show anomalous activation energies and temperature-dependent thresholds, which can be rationalised in this way. It makes physical sense: a dislocation which moves by climb-plus-glide in the interface between two dissimilar crystals (or a crystal and an amorphous solid such as silica) will do so at low stresses only if the atoms in both phases undergo small diffusive rearrangements as it passes.

This problem is analysed in the Appendix where it is shown that when the mobility of the dislocation in the particle–matrix interface is very restricted (so that all particles act at strong pinning points) the threshold stress increases to the "Orowan" stress [equation (41)] for boundary dislocations

$$\sigma_{tr} \approx \frac{0.8Gb_b}{l}. \tag{45}$$

But M depends on temperature [equation (44)] so that, over a range of temperature, M is neither high nor very restricted. Then the strain rate depends on stress and temperature in a complicated way (Appendix).

The results are illustrated in Figs 10 and 11. When no particles are present, creep follows the continuum equation [equation (3)]. With particles, the material behaviour at low stresses depends on the value of Q_i/RT. When T is low or Q_i large, the dislocation cannot move in the particle–matrix interface; then the Orowan threshold [equation (45)] must be exceeded for creep to occur. If, instead, Q_i/RT is very small, motion in the interface is easy and the lower threshold [equation (42)] applies. In either limit, the material behaves like a Bingham solid, such that

$$\dot{\varepsilon} \propto (\sigma - \sigma_{tr}). \tag{46}$$

For intermediate values of Q_i/RT the curves are non-linear and lie in between the two limits approaching the lower one at high stresses.

The expected temperature dependence of the creep rate is shown in Fig. 11. With decreasing temperature the activation energy changes from that for diffusion to that for motion in the interface. At low temperatures the activation energy is very sensitive to the applied stress, because the stress determines the number of particles which have to be bypassed by interfacial motion, which is the rate-controlling step at all but the highest temperatures.

There is one further complication. As creep proceeds, particles tend to accumulate on the boundaries from which matter is removed—those under compression [24, 39]. A strain $\gamma = 2\varepsilon$ removes a volume $(\gamma/2)d$ from these boundaries. All the particles previously contained in this volume, plus those with centres lying within the particle radius r on either side of the boundary plane,

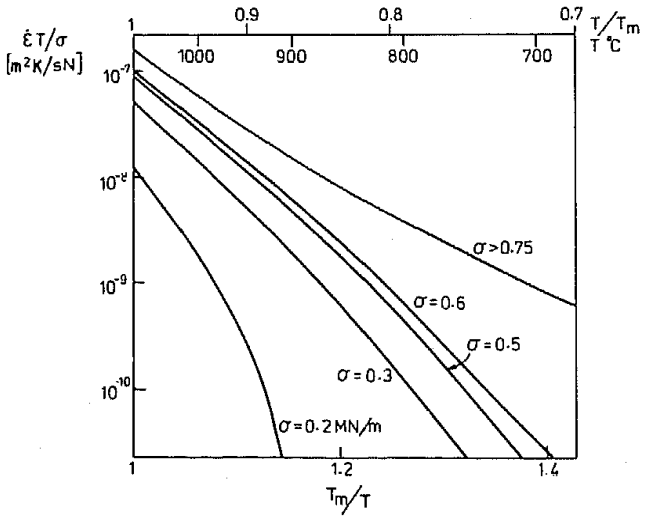

Fig. 11. The influence of grain boundary particles on the temperature dependence of diffusional creep, as predicted by equations (A5)–(A8). The parameter shown is the stress in MN m^{-2}.

Table 2. Apparent threshold stresses for creep in pure metals

Material	Grain size (μm)[a]	Temperature (K)	σ_{tr} (MN/m^2)[b]	σ_{tr}/G[c]	References
Cd	80 → 300	300	0.2	7.5×10^{-6}	Crossland [40]
Mg	25 → 170	425 → 596	0.88 → 0.09	$6 \times 10^{-5} \rightarrow 6 \times 10^{-6}$	Crossland and Jones [41]
Ag	40 → 220	473 → 623	1.0 → 0.3	$4 \times 10^{-5} \rightarrow 1.3 \times 10^{-5}$	Crossland [42]
Cu	35	523 → 573	0.6 → 0.4	$1.5 \times 10^{-5} \rightarrow 1 \times 10^{-5}$	Crossland [42]
Ni	130	1023	0.2	3.5×10^{-6}	Towle [43]
α-Fe	53 → 89	758 → 1073	0.3 → 0.05	$6 \times 10^{-6} \rightarrow 1 \times 10^{-6}$	Towle and Jones [44]
β-Co	35 → 206	773 → 1113	1.4 → 0.6	$9 \times 10^{-6} \rightarrow 1.7 \times 10^{-5}$	Sritharan and Jones [45]

[a] Grain size = 1.65 × mean linear intercept.
[b] Threshold stress in shear ($\sigma_{tr} = \sigma_0/\sqrt{3}$ when the tensile threshold σ_0 is given).
[c] Shear moduli at the test temperature calculated from data listed by Frost and Ashby [46].

intersect it. The number of obstacles per unit area, N_A is then

$$N_A = \left(\frac{\gamma d}{2} + 2r\right) N_V \tag{47}$$

where N_V is the number of particles per unit volume; if f is their volume fraction, then

$$N_V = \frac{3f}{4\pi r^3} \tag{48}$$

so that

$$N_A = \frac{3(\gamma d + 4r)f}{8\pi r^3}. \tag{49}$$

The mean spacing is now given by

$$l = N_A^{-1/2} = \left[\frac{8\pi r^3}{3f(\gamma d + 4r)}\right]^{1/2}. \tag{50}$$

This leads to a creep rate which decreases as deformation proceeds.

4. COMPARISON WITH EXPERIMENT

4.1. Pure materials

Data for diffusional creep in pure metals and ceramics are often well described by the continuum equation with which this paper started [equation (3)]; discrepancies can usually be explained by the difficulty of measuring d accurately, and by poor data for δD_b. This agreement is consistent with the model developed here: when the dislocation density is adequate, and their mobility is high, the rate-equations all reduce to that of the continuum model.

The model does, however, predict a threshold stress of general magnitude [equation (22)]

$$\sigma_0 \approx \frac{1}{2}\frac{b_b}{d} G.$$

Data for threshold stresses in nominally pure materials are assembled in Table 2. They are generally small, of order $10^{-5}\,G$. If b_b is set equal to $\frac{1}{3}b$ (the Burgers' vector of the crystal) then the threshold stresses predicted by this equation are about right.

4.2. Solid solutions

The diffusional creep of solid solutions is described by equations (37) and (38), and illustrated by Figs 12 and 13. When solute drag limits the mobility of the boundary dislocations, the stress exponent increases from 1 to 2 (Fig. 12), and the activation energy, even in the regime of Coble creep, reflects solute diffusion in the lattice rather than boundary diffusion (Fig. 13). At low temperatures and stresses, the creep rate can be extremely sensitive to impurity concentration (Fig. 13).

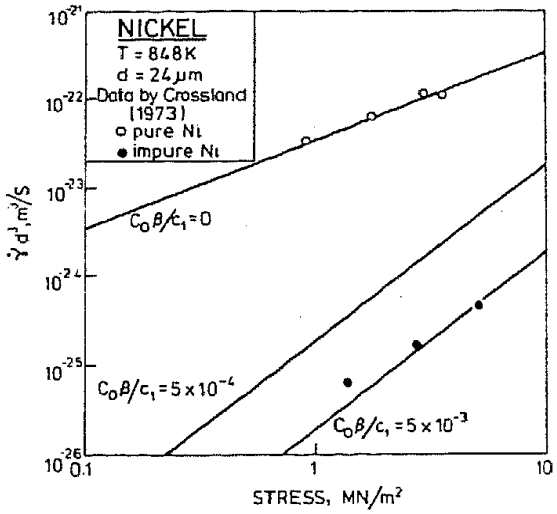

Fig. 12. The influence of solute on the stress dependence of diffusional creep, as predicted by equation (37) (C_0 is the solute concentration); experimental data by Crossland [42].

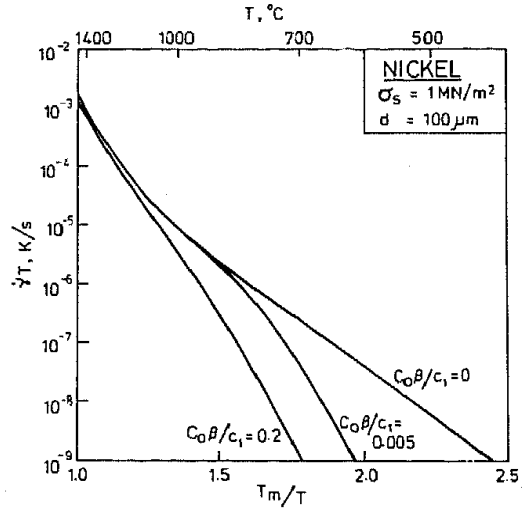

Fig. 13. The influence of solute on the temperature dependence of diffusional creep, as predicted by equation (37) (C_0 is the solute concentration). Lattice self-diffusivity was used for the solute diffusivity.

This is in broad agreement with experiments. Crossland [42] and Burton *et al.* [47] studied the effect of impurities on diffusional flow in nickel. They found that creep rates in commercial purity (99.5%) nickel were two to three orders of magnitude smaller than in high-purity nickel. The stress exponent, 1 in the high purity material, changed to 2, the activation energy from 120 kJ/mol to 280 kJ/mol (compared with 115 and 284 kJ/mol for grain boundary and lattice diffusion, respectively [46]).

If the parameter $C_0\beta/C_1$ of equation (37) is set equal to 0.005, corresponding to an impurity content $C_0 = 0.5\%$ with reasonable values for β and C_1, good agreement is found (Fig. 12). The temperature dependence shown in Fig. 13, too, is qualitatively confirmed by the results of Burton *et al.* [47]. Similar behaviour is found in zircaloy II, which, under conditions favouring grain boundary diffusion in pure zirconium, exhibits a temperature dependence characteristic of lattice diffusion [48].

The theory predicts a change in the grain size dependence of the creep rate from $\dot{\varepsilon} \propto (1/d^2)$ or $1/d^3$ to $\dot{\varepsilon} \propto (1/d)$ with increasing solute content. Such behaviour is observed in Al_2O_3 containing Ti and Mg as impurities [49]. It also appears to be typical of superplastic materials. Superplasticity occurs generally in fine-grained two-phase alloys, each phase containing a saturated solution of the other. In their rather complicated mechanical behaviour it is difficult to isolate the influence of the solute atoms, but for many superplastic alloys the strain rate $\dot{\varepsilon}$ is proportional to σ^2 [50–52]; and many show $\dot{\varepsilon} \propto \sigma^2/d$ as equation (38) predicts: examples are Al–33% Cu [53], Pb–Sn [54], Al–Zn [55], Sn–5% [56], the last three of which were replotted by Rai and Grant [53] on axes of σ vs $(\dot{\varepsilon}d)^{1/2}$ to demonstrate this.

In summary, the idea that a solute or impurity drag limits the mobility of grain-boundary dislocations seems to have merit. In particular, it explains the observation that, for many alloys, $\dot{\varepsilon} \propto \sigma^2/d$ and that the strain rate can be very sensitive to impurity content.

4.3. *Materials containing dispersed particles*

Particles increase the apparent threshold for diffusional flow† (Table 3), and increase the apparent activation energy (Table 4). The apparent stress exponent rises, and can be come very large (e.g. 40).

The earliest reports of an influence of particles on diffusional flow are on a two-phase hydrided Mg–0.5% Zr alloy subjected to low stresses [66]; particle-free zones were found on grain boundaries normal to the applied stress and particle accumulations on longitudinal grain boundaries. (Harris and Jones [67] subsequently showed that the strain rates could be inferred from the width of the precipitate-free zones.)

†It is often difficult, in these materials, to distinguish diffusional flow from power-law creep. The most reliable indication of diffusional flow is the grain-size dependence. We have selected data for which there was evidence of diffusional flow.

Table 3. Apparent threshold stresses for creep in alloys and ceramics

Material	Vol. FR (%)	Grain size (μm)	Temperature (K)	σ_{tr} (MN/m^2)[a]	σ_{tr}/G[b]	Reference
Ni–ThO_2	2	1.3/25	1365	31	6×10^{-4}	Whittenberger [57]
Ni–Cr–Al–ThO_2	2	150/490	1365	30	5×10^{-4}	
Ni–Cr–Al–ThO_2	2	120/1200	1365	24	4×10^{-4}	
INCONEL MA-754 Y_2O_3	0.6	115/130	1365	$10 \rightarrow 42$	$2 \times 10^{-4} \rightarrow 8 \times 10^{-4}$	
Ni–Cr–Al–Y_2O_3	1	310/2500	1366	24	4×10^{-4}	Whittenberger [58]
INCONEL MA-757–Y_2O_3	0.6	70/265	$1144 \rightarrow 1477$	$12 \rightarrow 52$	$2 \times 10^{-4} \rightarrow 9 \times 10^{-4}$	
Ni–Cr–ThO_2	2	—	$1173 \rightarrow 1473$	—	9×10^{-4}	Lund and Nix [59]
Cu–Al_2O_3	$0.5 \rightarrow 1.5$	13	1173	$0.3 \rightarrow 0.9$	$1 \times 10^{-5} \rightarrow 3.4 \times 10^{-5}$	Burton [11]
Cu–SiO_2	~2	34	$816 \rightarrow 1118$	~0.3	$\sim 10^{-5}$	Clegg and Martin [28]
Au–Al_2O_3	6.1	—	~1000	0.2	1.3×10^{-5}	Sautter and Chen [61]
	7.9	—	~1000	0.3	1.7×10^{-5}	
Stainless Steel–Nb (C, N)	0.3	14	~1000	$1 \rightarrow 2.6$	$2 \times 10^{-5} \rightarrow 5 \times 10^{-5}$	Crossland and Clay [62]
Stainless Steel–TiN	~5		1023	$30 \rightarrow 40$	$6 \times 10^{-4} \rightarrow 8 \times 10^{-4}$	Evans and Knowles [63]
UO_2-voids	3	7	$1523 \rightarrow 1723$	$2 \rightarrow 8.5$	$3 \times 10^{-4} \rightarrow 1 \times 10^{-4}$	Burton and Reynolds [64]
Mg–ZrH_2	—	18	723	0.5	3.9×10^{-5}	Karim and Backofen [65]

[a] Threshold stress in shear ($\sigma_{tr} = \sigma_0/\sqrt{3}$ when the tensile threshold σ_0 is given).
[b] Shear moduli at the test temperature calculated from data listed in Frost and Ashby [46].

Table 4. Activation energies in dispersion-strengthened materials

Material	Q for pure material (kJ/mol)	Q for DS-material (kJ/mol)	Reference
Cu + Al_2O_3	200	~500	Burton [11] (Nabarro–Herring creep)
Cu + SiO_2	105	~277	Clegg and Martin [28] (Coble Creep)
Stainless steel + TiN	280	~400	Evans *et al.* [72]
Mg–MgO (sintered)	134	~400	Vickers and Greenfield [70]
Al + Al_3Fe	145	~600	Barrett *et al.* [73]
Fe–3%Si + Al_2O_3	220	~600	Stang and Barrett [74]

The hydride particles reduced creep rates by up to two orders of magnitude [39, 68]. In sintered magnesium and Mg alloys containing MgO [69, 70, 39] the creep rates were reduced by up to seven orders of magnitude and the activation energy increased up to 250–400 kJ/mol, compared with 300 kJ/mol for diffusion of O in MgO [71].

All these observations are qualitatively consistent with the model. Note particularly the apparent suppression of diffusional creep (dotted line in Fig. 10b) as observed [39] in Mg–Zr H_2.

Stang and Barrett [74] found creep in P.M. Fe–3% Si containing 1 wt% Al_2O_3 to be slower than in single phase Fe–3% Si by about an order of magnitude. The inhibiting effect was strongly temperature dependent, with an apparent activation energy of about 600 kJ/mol (instead of 220 for single phase material) and a stress exponent slightly greater than 1. These facts can be qualitatively explained by the model. A similar reduction of creep rate was found [73] in Al + 0.5% Fe.

A threshold stress for diffusional creep was observed by Sautter and Chen [61] in Au containing dispersed Al_2O_3 particles. Figure 14 shows that the model can account for their results very well; only the activation energy Q_i for interfacial motion had to be adjusted, giving $Q_i = 355$ kJ/mol (which compares with 380 kJ/mol for boundary diffusion of the oxygen ion in Al_2O_3 [46]). We have been less successful in explaining

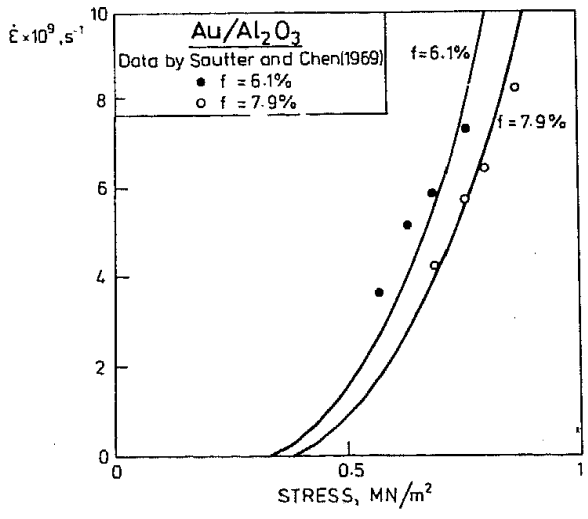

Fig. 14. Theory vs experimental results of Sautter and Chen [61] on Au/Al_2O_3 ($T = 1223$ K, $d = 40$ μm, $r = 0.5$ μm, $Q_i = 355$ kJ/mol).

quantitatively the creep behaviour of Cu/Al_2O_3 as measured by Burton [11]; if the grain size is stated correctly, the creep rates of Cu/Al_2O_3 at the high stresses seem to exceed those of pure copper.

In oxide-dispersion-strengthened (ODS) superalloys the inhibiting effect of inert particles on diffusional creep is very pronounced. Whittenberger [57, 58] for instance, found threshold stresses of the order of 10 MN m^{-2} in ODS Ni-based superalloys (see Table 3). In these mechanically alloyed materials the particle spacings are typically 0.15 μm [75]. These thresholds are well within the range predicted by the model (assuming the mobility in the interface to be very restricted)

$$\sigma_{tr} = \frac{0.8Gb_b}{l} \approx 30 \text{ MN m}^{-2}.$$

At stresses lower than the threshold stress, creep degradation due to the formation of dispersoid-free zones along grain boundaries normal to the applied stress, is suppressed [76]; clearly an understanding of threshold stresses in ODS alloys could be of practical importance.

Several studies report threshold stresses which depend strongly on temperature (e.g. Burton [11]; Clegg and Martin [28]). An explanation for this behaviour may be found in Fig. 10(a). At very low strain rates the creep curves show pronounced curvature; if these slow rates cannot be measured, then a linear extrapolation to low stresses gives the false impression of a temperature-dependent threshold stress. It still remains difficult to explain why the threshold stress is sometimes observed to drop to zero at the melting point [11]. Quantitative agreement with experimental data on Cu/SiO_2 [28] could only be obtained by using a threshold stress which was an order of magnitude lower than the measured particle spacing would imply. Neither inaccuracy in measuring the particle spacing, nor particle coarsening can provide an explanation. It may be that pile-ups of grain boundary dislocations form at the higher temperatures: if a pile-up of N dislocations forms between each opaque gate (Fig. 8, right) then the threshold stress can be reduced by a factor $1/N$. Such pile-ups have been invoked by Clegg and Martin [28] whose model resembles that developed here for the case of negligible threshold stresses.

In summary, creep retardation and threshold stresses in particle-strengthened materials can be understood in terms of the pinning of grain boundary dislocations. Qualitative agreement of the theory with experimental results was obtained, but the comparison seems to indicate that in some cases the threshold stresses can be lower than predicted by the theory.

5. SUMMARY AND CONCLUSIONS

The theory of diffusional flow ("Nabarro–Herring–Coble creep") is extended to include the details of the dislocation-like defects which act as the sinks and sources for matter. It is shown that the rate of creep depends on the density and mobility of these defects. Constitutive laws for the deformation are developed.

In the limit of pure materials of normal grain size, the laws all reduce to the classical equation for diffusional flow. But when impurities or solutes exert a drag on the defects, or particles pin them, the characteristics of the deformation change: the stress dependence becomes stronger; threshold stresses may appear below which creep rates become negligible; and the apparent activation energy for creep may increase.

These effects are analysed in detail, and wherever possible, compared with experimental data. Good qualitative agreement is found. The model appears to offer an explanation of many confusing experimental observations, although some still remain unexplained.

REFERENCES

1. H. Jones, *Mater. Sci. Engng* **4,** 106 (1969).
2. B. Burton, *Diffusional Creep of Polycrystalline Materials*, Trans. Tech., OH (1977).
3. W. Bollmann, *Crystal Defects and Crystalline Interfaces*. Springer, Berlin (1970).
4. G. H. Bishop and B. Chalmers, *Scripta metall.* **2,** 133 (1968).
5. M. F. Ashby, F. Spaepen and S. Williams, *Acta metall.* **26,** 1647 (1978).
6. R. C. Pond and V. Vitek, *Proc. R. Soc. Lond.* **A357,** 453 (1977).
7. D. A. Smith, R. C. Pond and V. Vitek, *Acta metall.* **25,** 475 (1977).
8. R. W. Balluffi (editor), *Grain Boundary Structure and Kinetics*. Am. Soc. Metals, Metals Park, OH (1980).
9. M. F. Ashby, *Scripta metall.* **3,** 837 (1969).
10. M. F. Ashby, *Surf. Sci.* **31,** 498 (1972).
11. B. Burton, *Metal Sci. J.* **5,** 11 (1971).
12. H. Gleiter, *Acta metall.* **17,** 565 (1969).
13. T. Schober and R. W. Balluffi, *Phil. Mag.* **21,** 109 (1970).
14. F. R. N. Nabarro, *Bristol Conf. on Strength of Solids*, p. 75 (1948).
15. C. Herring, *J. appl. Phys.* **21,** 437 (1950).
16. I. M. Lifshitz, *Soviet Phys. J.E.T.P.* **17,** 909 (1963).
17. R. L. Coble, *J. appl. Phys.* **34,** 1679 (1963).
18. G. B. Gibbs, *Mém scient. Revue Métall.* **62,** 781 (1965).
19. R. Raj and M. F. Ashby, *Trans. Am. Inst. Min. Engrs* **2,** 1113 (1971).
20. J. P. Hirth and J. Lothe, *Theory of Dislocations*, p. 522. McGraw-Hill, New York (1968).
21. A. M. Brown and M. F. Ashby, *Acta metall.* **28,** 1085 (1980).
22. B. Burton, *Mater. Sci. Engng* **10,** 9 (1972).
23. G. W. Greenwood, *Scripta metall.* **4,** 171 (1970).
24. B. Burton, *Mater. Sci. Engng* **11,** 337 (1973).
25. J. E. Harris, *Metal Sci. J.* **7,** 1 (1973).
26. B. Burton and W. B. Beeré, *Metals Sci.* **12,** 71 (1978).
27. B. Burton and W. B. Beeré, *Phil. Mag.* **43,** 1561 (1981).
28. W. J. Clegg and J. W. Martin, *Metals Sci.* **16,** 65 (1982).
29. D. Lazarus, *Encyclopedia of Science and Technology*, p. 158. McGraw-Hill, New York (1971).
30. I.-W. Chen, *Acta metall.* **30,** 1317 (1982).
31. A. H. Cottrell and M. A. Jaswon, *Proc. R. Soc.* **A199,** 104 (1949).
32. A. H. Cottrell, *Dislocations and Plastic Flow in Crystals*. Oxford Univ. Press (1953).
33. J. Friedel, *Dislocations*, p. 356. Addison-Wesley, Reading, MA (1964).
34. W. K. Burton, N. Cabrera and F. C. Frank, *Phil. Trans. R. Soc. Lond.* **A243,** 299 (1951).
35. U. F. Kocks, *Phil. Mag.* **13,** 541 (1966).
36. R. S. W. Shewfelt and L. M. Brown, *Phil. Mag.* **35,** 945 (1977).
37. E. Arzt and M. F. Ashby, *Scripta metall.* **16,** 1285 (1982).
38. M. F. Ashby and R. M. A. Centamore, *Acta metall.* **16,** 1081 (1968).
39. J. E. Harris, R. B. Jones, G. W. Greenwood and M. J. Ward, *J. Aust. Inst. Metals* **14,** 154 (1969).
40. I. G. Crossland, *Physica status solidi* **A23,** 231 (1974).
41. I. G. Crossland and R. B. Jones, *Metals Sci.* **11,** 504 (1977).
42. I. G. Crossland, in *Physical Metallurgy of Reactor Fuel Elements* (edited by J. E. Harris and E. C. Sykes), p. 66. Metals Soc., London (1973).
43. D. J. Towle, Ph.D. Thesis, Univ. of Sheffield (1975).
44. D. J. Towle and H. Jones, *Acta metall.* **24,** 399 (1976).
45. T. Sritharan and H. Jones, *Acta metall.* **27,** 1293 (1979).
46. H. J. Frost and M. F. Ashby, *Deformation Mechanism Maps*. Pergamon Press, Oxford (1982).
47. B. Burton, I. G. Crossland and G. W. Greenwood, *Metals Sci.* **14,** 134 (1980).
48. I. M. Bernstein, *Trans. Am. Inst. Min. Engrs* **239,** 1518 (1967).
49. Y. Ikuma and R. S. Gordon, in *Surfaces and Interfaces in Ceramic and Ceramic–Metal Systems* (edited by J. Pask and A. Evans), p. 283. Plenum Press, New York (1981).
50. T. H. Alden, *Acta metall.* **15,** 469 (1967).
51. H. W. Hayden, R. C. Gibson, H. F. Merrick and J. H. Brophy, *Trans. Am. Metals Soc.* **60,** 3 (1967).
52. G. S. Murty, *Scripta metall.* **6,** 633 (1972).
53. G. Rai and N. J. Grant, *Metall. Trans.* **6A,** 385 (1975).
54. D. H. Avery and W. A. Backofen, *Trans. Am. Soc. Metals* **58,** 551 (1965).
55. D. L. Holt, *Trans. Am. Inst. Min. Engrs* **242,** 25 (1968).
56. T. H. Alden, *Trans. Am. Inst. Min. Engrs* **236,** 1633 (1966).
57. J. D. Whittenberger, *Metall. Trans.* **8A,** 1155 (1977).
58. J. D. Whittenberger, *Metall. Trans.* **12A,** 193 (1981).
59. R. W. Lund and W. D. Nix, *Acta metall.* **24,** 469 (1976).
60. R. S. W. Shewfelt and L. M. Brown, *Phil. Mag.* **30,** 1135 (1974).
61. F. K. Sautter and E. S. Chen, *Proc. 2nd Bolton Landing Conf. on Oxide Dispersion Strengthening*, p. 495. Gordon & Breach, New York (1969).
62. I. G. Crossland and B. D. Clay, *Acta metall.* **25,** 929 (1977).
63. H. E. Evans and G. Knowles, *Metals Sci.* **14,** 262 (1980).
64. B. Burton and G. L. Reynolds, *Acta metall.* **21,** 1073 (1973).
65. A. Karim and W. A. Backofen, *Metall. Trans.* **3,** 709 (1972).
66. R. L. Squires, R. T. Weiner and M. Phillips, *J. nucl. Mater.* **8,** 77 (1963).
67. J. E. Harris and R. B. Jones, *J. nucl. Mater.* **10,** 360 (1963).
68. P. Greenfield, C. C. Smith and A. M. Taylor, *Trans. Am. Inst. Min. Engrs* **221,** 1065 (1961).
69. P. Greenfield and W. Vickers, *J. nucl. Mater.* **22,** 77 (1967).
70. W. Vickers and P. Greenfield, *J. nucl. Mater.* **27,** 73 (1968).
71. Y. Oishi and W. D. Kingery, *J. chem. Phys.* **33,** 905 (1960).
72. H. E. Evans, D. Raynor, A. C. Roberts and J. M. Silcock, in *Microstructure and Design of Alloys, Proc. Third Int. Conf. on Strength of Metals and Alloys*, Vol. 1, p. 190 (1973).

73. C. R. Barrett, E. C. Muehleisen and W. D. Nix, *Mater. Sci. Engng* **10**, 33 (1972).
74. R. G. Stang and C. R. Barrett, *Scripta metall.* **7**, 233 (1973).
75. B. A. Wilcox and A. H. Clauer, *Acta metall.* **20**, 743 (1972).
76. J. D. Whittenberger, *Metall. Trans.* **4**, 1475 (1973).

APPENDIX

BY-PASSING OF BOUNDARY PARTICLES

We treat the problem using the general ideas of Shewfelt and Brown [36, 60] which we simplify and adapt for boundary dislocations. Consider unit length of boundary dislocation, traversing a boundary, and interacting with obstacles (which we think of as hard, inert particles) as it moves (Fig. 8). If the stress were sufficiently high, the dislocation could bow between, and by-pass all the obstacles without climbing over any of them. This stress (the "Orowan Stress") is

$$\sigma_{Or} = \frac{C_3 G b_b}{l} \tag{A1}$$

where $C_3 \approx 0.8$ (see, for example, Kocks [35]). The number of particles per unit length of the dislocation is

$$n = \frac{1}{l} = \frac{\sigma_{Or}}{C_3 G b_b}. \tag{A2}$$

Let the stress be less than σ_{Or}. Then creep is possible only if the dislocation climbs over some of the obstacles, allowing it to by-pass the remainder. The number it can by-pass is

$$n^* = \frac{\sigma}{C_3 G b_b} \tag{A3}$$

leaving at least $(n - n^*)$ particles which must be by-passed by climb if the dislocation is to move indefinitely. If climb is rapid—that is, the mobility in the interface is high—the strain rate may be higher if the dislocation climbs over a larger number of particles, because looping then occurs at a reduced Orowan stress $\sigma_{Or}(1 - n_c/n)$. The following consideration allows this effect to be incorporated.

Let the number of particles per unit length which are by-passed by climb be n_c. Equate the work done by the remote stress σ_s, acting on unit length of dislocation, to n_c times the change in elastic energy of the dislocation as it rides up over the particle, plus n_c times the viscous work done against its restricted mobility in the particle matrix interface, plus $(1 - n_c/n)$ times the work done in pushing the dislocation between $(1 - n_c/n)$ particles, plus the energy required to drive long range diffusion across the grain. If the dislocation advances by δx then

$$\sigma_s b \delta x = \left(E_s \delta l + \frac{2rv^2}{M_i}\delta t\right) n_c + \sigma_{Or} b \delta x \left(1 - \frac{n_c}{n}\right)^2 + \frac{\dot{\gamma}}{\dot{\gamma}_c}\sigma_s b \delta x. \tag{A4}$$

Here δl is the increase in line length as a segment of dislocation rides up over one particle of diameter $2r$, E_s is the elastic energy per unit length (roughly $Gb_b^2/2$), $v\,(= \delta x/\delta t)$ is the velocity of the dislocation, and δt is the time taken to move through δx. The last term $(\sigma b \delta x \dot{\gamma}/\dot{\gamma}_c)$ is the work required to drive long-range diffusion, where $\dot{\gamma}_c$ is the continuum limiting strain rate given by equation (3). Rearranging, and using $\dot{\gamma} = 2\rho b_b v/d$ gives

$$\dot{\gamma} = \dot{\gamma}_c \frac{\sigma_s - \sigma_{Or}\left[A\frac{n_c}{n} + \left(1 - \frac{n_c}{n}\right)^2\right]}{\sigma_s + \dot{\gamma}_c B \sigma_{Or} n_c/n} \tag{A5}$$

where

$$A = \left(\frac{dl}{dx}\right)\Big/ 2C_3 \tag{A6}$$

and

$$B = rd/C_3 M_i b_b^3 \rho G$$

and dl/dx measures the climb-stiffness of the obstacle; it has a mean value of 0.77 for spherical particles [37]. This strain rate is a maximum when the fraction of particles that are by-passed in the interface is

$$\frac{n_c}{n} = \sqrt{(s+1)^2 - (A + \dot{\gamma}_c B)s} - s \tag{A7}$$

where

$$s = \sigma_s/\sigma_{Or}\dot{\gamma}_c B. \tag{A8}$$

(The values of n_c/n must, of course, be limited to the range $[0, 1]$.)

If the mobility in the interface is low $(B \to \infty)$ then equation (A7) reduces to

$$\frac{n_c}{n} = \left(\frac{\sigma_{Or} - \sigma_s}{\sigma_{Or}}\right)^{1/2} \tag{A9}$$

which is close to, but always higher than the minimum number required to sustain looping, $1 - n^*/n$. If, on the other hand, the mobility is high $(B = 0)$, then

$$\frac{n_c}{n} = \frac{2 - A}{2} \tag{A10}$$

which is independent of stress. Note that in all cases, finite mobility $(B < \infty)$ implies that even above the Orowan stress, some particles will be by-passed by climb, because the strain rate is higher than it would be only for looping.

Equations (A5–A8) predict the shear strain rate, as a function of shear stress, when grain boundary dislocations can by-pass particles by looping as well as climb/glide in the particle/matrix interface. This set of equations

(a) reduces to the continuum limit, equation (3):

$$\dot{\gamma} = \dot{\gamma}_c \tag{A11}$$

when the particles are removed $(\sigma_{Or} = 0)$;

(b) predicts a maximum threshold stress

$$\sigma_{tr} = \sigma_{Or} \tag{A12}$$

when mobility in the interface is very low $(B \to \infty, n_c = 0, B \cdot n_c \to 0)$;

(c) predicts a lower threshold stress, typically

$$\sigma_{tr} \simeq \tfrac{1}{3}\sigma_{Or} \tag{A13}$$

when the mobility at the interface is high;

(d) predicts a high activation energy when the interfacial motion is rate controlling

$$\dot{\gamma} \propto \frac{D_i b \rho G}{kTrd}; \tag{A14}$$

(e) predicts more complicated behaviour, illustrated in Fig. 10, when the mobility in the particle–matrix interface is limited. This last case can have the characteristics of a temperature-dependent threshold stress, though it is not a true threshold.